

Giant Davydov splitting of the lower polariton branch in a polycrystalline tetracene microcavity

S. Kéna-Cohen¹ and S. R. Forrest^{2,*}¹*Princeton Institute for the Science and Technology of Materials (PRISM), Department of Electrical Engineering, Princeton University, Princeton, New Jersey 08544, USA*²*Departments of Electrical Engineering and Computer Science and Physics, University of Michigan, Ann Arbor, Michigan 48109, USA*
(Received 16 January 2008; published 25 February 2008)

We demonstrate strong exciton-photon coupling of Frenkel molecular excitons at room temperature in an all-metal microcavity containing a thin film of crystalline tetracene, with micron scale domains. In contrast to previous reports of strong coupling in organic microcavities containing localized excitonic states, here we observe large Davydov splitting of the lowest excited state, indicating strong, *intermolecular* interactions. The angle-resolved reflectivity of the microcavity is measured and understood in terms of the anisotropic dielectric constant of tetracene single crystals. The anisotropy leads to the formation of additional normal modes, and a giant splitting of the lower polariton branch is observed due to birefringence along both Davydov components.

DOI: [10.1103/PhysRevB.77.073205](https://doi.org/10.1103/PhysRevB.77.073205)

PACS number(s): 78.40.Me, 42.70.Jk

Organic semiconductors provide an interesting platform for the study of elementary excitations due to the strong interactions that may occur between electrons, holes, molecular vibrations, and the lattice. The tightly bound electron-hole pair which occurs in an organic molecular crystal upon optical excitation is called a Frenkel exciton.¹ The crystal periodicity and resonant intermolecular Coulomb interaction give rise to an excitonic band, and for crystals with more than one molecule per unit cell, the excitonic band is split into as many Davydov components as there are inequivalent molecules in the unit cell.² When a material possessing a strong excitonic resonance is placed inside a microcavity, it can strongly couple to the cavity photon to form a new elementary excitation called a cavity polariton.³ This occurs if the cavity photon and exciton dissipative widths are smaller than the coupling strength. Up until the present, there have been several observations of strong exciton-photon coupling in microcavities containing highly disordered or amorphous organic films of *J*-aggregates^{4–8} or low-molecular-weight organics.^{9,10} However, the largest fraction of excitations in disordered films in microcavities are localized, or “incoherent,” rather than polaritonic or “coherent” states.^{11–13} The localization of these excitations occurs mostly as a result of the disorder-induced inhomogeneous broadening of the excitonic transition and the absence of intermolecular interaction. Indeed, highly ordered or crystalline organic microcavities are of particular interest due to their potential for exploitation of nonlinear processes such as parametric amplification.^{11,14,15} Here, we demonstrate strong exciton-photon coupling in an all-metal microcavity containing a thin film of polycrystalline tetracene. This study is a demonstration of strong exciton-photon coupling in a crystalline organic microcavity where the intermolecular interaction is strong enough to exhibit a Davydov splitting up to room temperature. Indeed, Davydov splitting can only exist in the presence of an excitonic state that samples multiple molecules within a unit cell. In this case, the crystalline morphology is crucial to observing the giant splitting of the lower polariton branch due to birefringence along both Davydov components of the lowest excited state of tetracene. Indeed, our experimental results are consistent with previous theoretical descriptions of the excitation spectrum of crystalline organic microcavities,^{16,17} and confirm that the effects of

anisotropy are reduced by the presence of the microcavity. In general, the resulting polaritons are a coherent superposition of both photon polarizations, both Davydov components, and the three lowest vibronic bands of tetracene.

To our knowledge, there has only been one report of strong coupling in a polycrystalline organic thin film.¹⁸ In contrast to that work where no evidence for long range order was noted, we report here on a microcavity containing a tetracene film with crystalline domains several microns in diameter, i.e., much longer than an optical wavelength. In this case, the anisotropic dielectric function, whose origin lies in optical interactions with the individual macroscopic crystallites, must be employed to understand the observed polariton dispersion. Since the probe spot diameter (~ 1 mm) is much larger than the individual crystallites, the observed reflectivity consists of an average of the reflectivity of randomly oriented single crystal microcavities. The weak dependence of the excitation spectrum on azimuthal angle allows us to resolve the polariton dispersion. In addition, previous theoretical work has shown that both photon polarizations participate in the formation of the polaritonic state in anisotropic organic crystals, in contrast to inorganic quantum wells where the *s* and *p* polarizations are decoupled.^{16,17}

The microcavity structure consisted of a thin film of tetracene sandwiched between two Ag mirrors. The use of an all-metal cavity greatly increases the electric field intensity within the cavity compared to dielectric Bragg reflectors.¹⁹ However, this occurs at the cost of a lower cavity *Q* factor ($Q \sim 26$) due to loss at the metal mirrors. The bottom mirror consists of an 80 nm thick Ag film, deposited by vacuum thermal evaporation onto a Si (100) substrate. Tetracene film thicknesses ranging between 115 and 180 nm were used for the cavity material. The structure was capped by a 35 nm thick Ag top mirror.

The source tetracene was purified twice by gradient sublimation prior to use. Films were deposited by thermal sublimation in a vacuum of 10^{-7} Torr onto substrates consisting of thermally evaporated Ag films on Si (100), SiO₂ on Si (100), and quartz. In all cases, the substrates were held at room temperature during deposition. Polarized optical micrographs taken under white-light illumination are shown in Figs. 1(a) and 1(b) for 115 nm tetracene films grown simultaneously on both Ag and SiO₂. The polycrystalline nature of

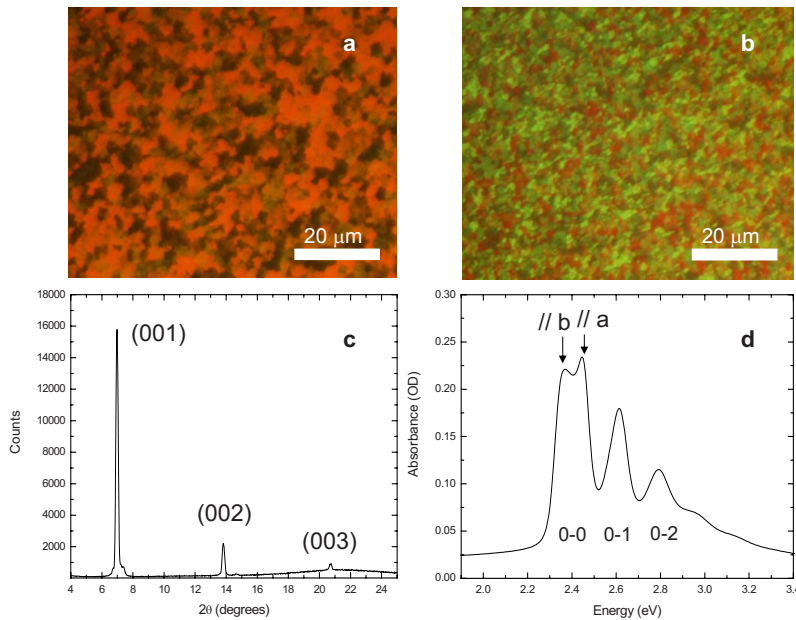


FIG. 1. (Color online) Optical micrographs of a 115 nm thick tetracene film taken through crossed polarizers are shown for tetracene simultaneously deposited on (a) 80 nm thick thermally evaporated Ag and (b) SiO_2 . The scale bar corresponds to 20 μm . (c) $\text{Cu K}\alpha$ Bragg-Brentano x-ray diffraction data confirming the crystalline nature of the film. Multiple diffraction orders are seen. Stacking occurs in the (001) direction, with the ab planes lying parallel to the substrate. The broad peak near $\sim 21^\circ$ is due to the quartz substrate. (d) Absorbance of a 140 nm thick tetracene film sublimed onto a quartz substrate. The two Davydov components and the three lowest vibronic transitions are identified.

the films is clearly visible on both substrates. The domain size was found to vary significantly with growth rate (0.2–5 $\text{\AA}/\text{s}$), and is typically on the order of 1–10 μm , with slow deposition resulting in larger grains. X-ray diffraction patterns taken in the Bragg-Brentano configuration [Fig. 1(c)] confirm the triclinic structure of the tetracene thin films and previous reports that stacking on SiO_2 occurs in the (001) direction with the ab plane lying parallel to the substrate.^{20,21} Molecular stacking on Ag also occurs in the (001) direction, and for films grown under identical conditions, the grains are typically larger on Ag than on SiO_2 by 2–3 μm . This is likely due to a slower nucleation rate for tetracene on Ag as compared to SiO_2 . Prior to top mirror deposition, the film roughness was measured to be 8 nm by atomic force microscopy.

The absorption spectrum of a 140 nm thick tetracene film deposited on a quartz substrate is shown in Fig. 1(d). The tetracene p band²² is characterized by two strong absorption resonances at $E_{0-0a}=2.467$ eV and $E_{0-0b}=2.384$ eV that are polarized along a and b , respectively.²³ The splitting of this transition, called the Davydov splitting, occurs due to the resonant Coulomb interaction between the two molecules comprising the tetracene unit cell.² The 0-1 ($E_{0-1}=2.610$ eV) and 0-2 ($E_{0-2}=2.801$ eV) vibronic bands of tetracene are of comparable strength to the 0-0 band, and also possess different oscillator strengths along the a and b directions. Although the crystalline domains are rotationally isotropically oriented, a manifestation of the crystalline nature of the films is directly observed in their absorption spectra. Since the crystallites are transparent to light polarized along a at energy E_{0-0b} , which corresponds to the transition with the strongest oscillator strength, the absorption of this resonance is limited to 50% regardless of the film thickness.²⁰

Room temperature angle-resolved reflectivity for the cavity containing a 160 nm thick tetracene layer is shown in Fig. 2(a) for s -polarized light. The positions of the uncoupled resonances are indicated by dashed lines. The presence of

two lower polariton (LP) branches separated by $\Delta E_{\text{LP}}=243$ meV at 15° , and identified by the labels LP_a and LP_b , are clearly visible at low energy. The two lower branches follow the usual inverse cosine cavity photon dispersion⁹ at low angle, θ . At $\theta\sim 40^\circ$, the lowest energy branch (LP_b) anticrosses around the E_{0-0b} resonance, while the LP_a branch anticrosses around the E_{0-0a} resonance. As shown below, the local anisotropy must be considered to understand the splitting of the lower branch despite the random azimuthal orientation of the crystallites on the scale of the probe spot diameter.

Also note the presence of hybrid modes (HP) located between the E_{0-0} , E_{0-1} , and E_{0-2} vibronics. These modes are a coherent superposition of the cavity photon and the three strongest vibronic bands. The mixing of intramolecular vibronics was previously observed for the two lowest vibronics of 3,4,7,8 naphthalenetetracarboxylic dianhydride, and was understood in terms of a coupled-mode formalism.¹⁸ At higher incident angles ($\theta>45^\circ$), the upper polariton (UP) branch energy increases with angle. It acquires a broad, three-peak structure as it crosses the weak E_{0-3} vibronic, and the birefringence causes the UP_a and UP_b components to separate slightly. However, the birefringence is much smaller at high energy than it is on the low energy side of the excitonic resonances. This makes it difficult to distinguish between UP_a and UP_b .

In addition to the splittings caused by the birefringence, a polarization splitting occurs due to the different phase change for s - and p -polarized light reflected from metal mirrors with finite loss. This is due to a splitting in the photon component of the cavity. To simplify the discussion, we only consider s -polarized reflectivity. We have reproduced the experimental results by calculating the reflectivity using a transfer matrix scheme that consists in diagonalizing Berreman's 4×4 matrix.^{24,25} The dielectric tensor for a tetracene crystallite, where the principal axis is at an angle ϕ with the laboratory frame x axis, can be written as

$$\varepsilon_{ij}(\omega) = \begin{pmatrix} \varepsilon_a(\omega)\cos^2\phi + \varepsilon_b(\omega)\sin^2\phi & \cos\phi\sin\phi[\varepsilon_a(\omega) - \varepsilon_b(\omega)] & 0 \\ \cos\phi\sin\phi[\varepsilon_a(\omega) - \varepsilon_b(\omega)] & \varepsilon_a(\omega)\sin^2\phi + \varepsilon_b(\omega)\cos^2\phi & 0 \\ 0 & 0 & \varepsilon_c \end{pmatrix}, \quad (1)$$

where ω is the frequency of the incident light, and ε_a and ε_b are the single crystal dielectric constants along a and b , respectively. Since reflectivity must be averaged over all azimuthal angles, we have taken the unit cell as cubic to simplify calculations. The experimentally reported triclinic angle (γ) is 86.3° .²¹ Both dielectric constants were modeled as a sum of three Lorentz oscillators representing the three lowest energy vibronics, with the E_{0-2} contribution assumed to be isotropic. The uncoupled energies, linewidths, and oscillator strengths were taken from single crystal values reported previously.^{26,27} A simple pole of amplitude $A=0.192$ was included at high energy ($E_\alpha=5.72$ eV) to account for α and β band absorption. Since the dependence on ε_c is very weak for s -polarized light, we assume a constant value of $\varepsilon_c=2.42$.

Figure 2(b) shows the reflectivity spectra calculated for the cavity containing the 160 nm thick tetracene film. All of the significant features generated from our model are consistent with observation. The experimentally determined upper branch is much broader than in simulations due to the exclusion of the higher energy vibronics from the assumed refractive index. The other principal source of experimental line broadening occurs from assuming only a single cavity thickness, while the grown film has a pronounced surface roughness. Finally, the birefringence in the transparent region of the spectrum (at $E < 2.2$ eV) needed to fit the lower branch splitting is determined to be $\Delta n \sim 0.2$ from simulations, in agreement with previous reports.²⁸

Reflectivities were also calculated for cavity thicknesses of 115, 140, 160, and 180 nm using the same dielectric tensor elements. The approximate dispersions extracted from contour plots of the simulated reflectivity are shown in Fig. 3. The superimposed black circles correspond to experimen-

tally determined peak positions for cavities of the same thicknesses. The simulation results are once again consistent with experiment. The dispersions are approximate since the distinction between the longitudinal and transverse components of the in-plane wave vector (k_{\parallel}) is lost after averaging. Although the effects of anisotropy are reduced by the presence of the microcavity, the important spectral features are, nevertheless, preserved by the averaging process. For $k_{\parallel} \ll k$ (where $k^2 = k_x^2 + k_y^2 + k_z^2 = k_{\parallel}^2 + k_z^2$), the dispersion of the branches corresponding to the two Davydov components is nearly independent, which is consistent with previous theoretical predictions.^{16,17} This is apparent in the distinct anticrossing behavior of both lower branches. For these branches, the azimuthal angle dependence of the dispersion is weak, and on the order of k_{\parallel}^2/k^2 . Hence, averaging over angle only leads to a small effective broadening of these branches.

In conclusion, we have demonstrated strong exciton-photon coupling in a microcavity containing a polycrystalline film of tetracene. This study is a demonstration of strong coupling in an organic microcavity containing crystalline domains on the micron scale, thus significantly exceeding the wavelength of the incident beam. The coherent nature of the delocalized excitations in tetracene results in a Davydov splitting, which can be observed up to room temperature. This, in turn, leads to a giant birefringence-induced splitting of the lower polariton branch. The reflectivity spectrum is found to be an azimuthal angular average of the reflectivity of tetracene single crystal microcavities. These results are consistent with previous theoretical investigations of the excitation spectrum of crystalline organic microcavities.^{16,17} Due to the high degree of crystalline order and the presence of significant intermolecular interaction, this type of structure is an important step toward the exploitation of nonlinear optical processes in organic microcavities.¹⁴

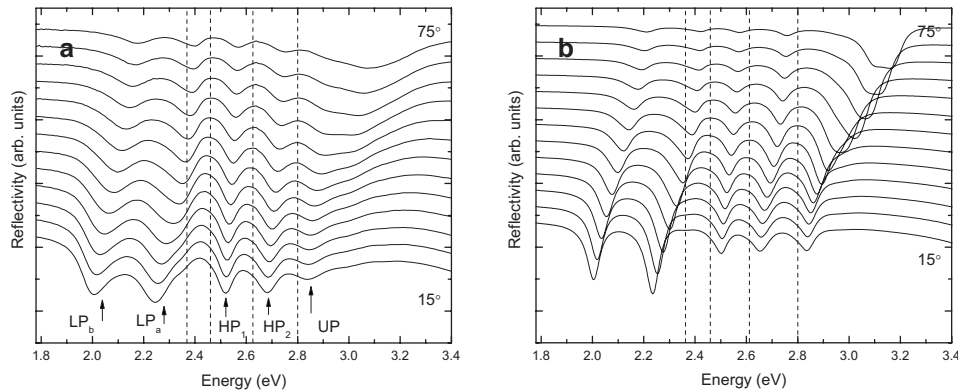


FIG. 2. (a) The angle-dependent reflectivity spectrum of a microcavity containing a 160 nm thick tetracene film. The spectra are taken in 5° increments. The dotted lines indicate the energies of the bare resonances observed in the absence of a cavity. Positions of the two lower polariton branches (LP), hybrid branches (HP), and upper branch (UP) are indicated. (b) Simulated reflectivity of the microcavity in (a) using the anisotropic transfer matrix scheme described in text. The reflectivities are averaged over all possible azimuthal angles.

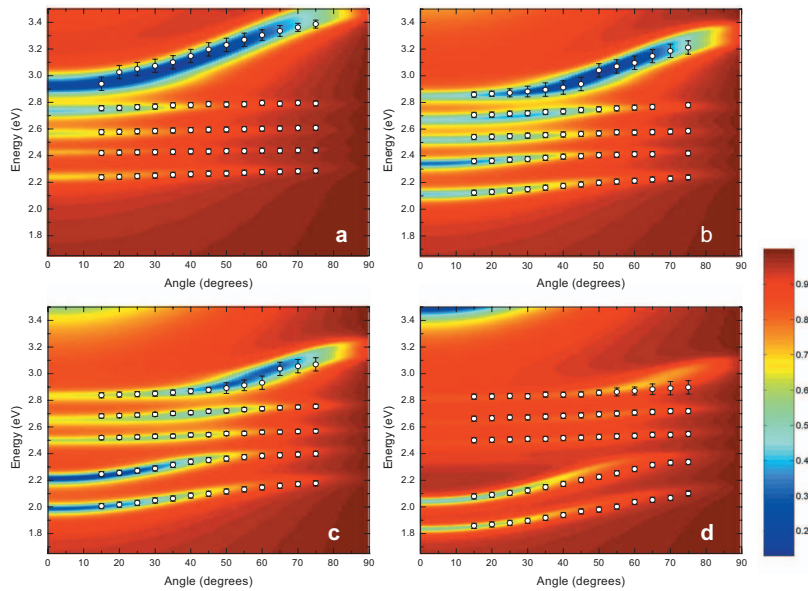


FIG. 3. (Color) Contour plots are of the simulated average s -polarized reflectivity of microcavities containing tetracene thicknesses of (a) 115 nm, (b) 140 nm, (c) 160 nm, and (d) 180 nm. The reflectivity is calculated using the procedure in Fig. 2(b). Reflectivity values are specified by the color bar. The black circles correspond to the experimental peak positions extracted from the reflectivity of cavities of the same thickness.

The authors acknowledge helpful discussions with Vladimir Agranovich and Marcelo Davanco. We also thank Universal Display Corp. and the Air Force Office of Scien-

tific Research for partial financial support of this work. S.K.C. acknowledges support from the Fonds Québécois sur la Nature et les Technologies.

*Author to whom correspondence should be addressed; stevefor@umich.edu

¹J. Frenkel, Phys. Rev. **37**, 17 (1931).

²A. S. Davydov, *Theory of Molecular Excitons* (Plenum, New York, 1971).

³C. Weisbuch, M. Nishioka, A. Ishikawa, and Y. Arakawa, Phys. Rev. Lett. **69**, 3314 (1992).

⁴J. H. Song, Y. He, A. V. Nurmikko, J. Tischler, and V. Bulovic, Phys. Rev. B **69**, 235330 (2004).

⁵P. Schouwink, J. M. Lupton, H. von Berlepsch, L. Dahne, and R. F. Mahrt, Phys. Rev. B **66**, 081203(R) (2002).

⁶D. G. Lidzey, A. M. Fox, M. D. Rahn, M. S. Skolnick, V. M. Agranovich, and S. Walker, Phys. Rev. B **65**, 195312 (2002).

⁷D. G. Lidzey, D. D. C. Bradley, T. Virgili, A. Armitage, M. S. Skolnick, and S. Walker, Phys. Rev. Lett. **82**, 3316 (1999).

⁸D. G. Lidzey, D. D. C. Bradley, A. Armitage, S. Walker, and M. S. Skolnick, Science **288**, 1620 (2000).

⁹D. G. Lidzey, D. D. C. Bradley, M. S. Skolnick, T. Virgili, S. Walker, and D. M. Whittaker, Nature (London) **395**, 53 (1998).

¹⁰R. J. Holmes and S. R. Forrest, Phys. Rev. B **71**, 235203 (2005).

¹¹M. Litinskaya and P. Reineker, Phys. Rev. B **74**, 165320 (2006).

¹²V. M. Agranovich, M. Litinskaia, and D. G. Lidzey, Phys. Rev. B **67**, 085311 (2003).

¹³V. M. Agranovich and Y. N. Gartstein, Phys. Rev. B **75**, 075302

(2007).

¹⁴H. Zoubi, Phys. Rev. B **74**, 045317 (2006).

¹⁵P. G. Savvidis, J. J. Baumberg, R. M. Stevenson, M. S. Skolnick, D. M. Whittaker, and J. S. Roberts, Phys. Rev. Lett. **84**, 1547 (2000).

¹⁶H. Zoubi and G. C. La Rocca, Phys. Rev. B **71**, 235316 (2005).

¹⁷M. Litinskaya, P. Reineker, and V. M. Agranovich, Phys. Status Solidi A **201**, 646 (2004).

¹⁸R. J. Holmes and S. R. Forrest, Phys. Rev. Lett. **93**, 186404 (2004).

¹⁹P. A. Hobson, W. L. Barnes, D. G. Lidzey, G. A. Gehring, D. M. Whittaker, M. S. Skolnick, and S. Walker, Appl. Phys. Lett. **81**, 3519 (2002).

²⁰W. Hofberger, Phys. Status Solidi A **30**, 271 (1975).

²¹R. B. Campbell, J. Trotter, and J. Monteath, Acta Crystallogr. **15**, 289 (1962).

²²E. Clar, *Polycyclic Hydrocarbons* (Academic, London, 1964).

²³A. Bree and L. E. Lyons, J. Chem. Soc. **1960**, 5206.

²⁴M. Schubert, Phys. Rev. B **53**, 4265 (1996).

²⁵D. W. Berreman, J. Opt. Soc. Am. **62**, 502 (1972).

²⁶J. Tanaka, Bull. Chem. Soc. Jpn. **38**, 86 (1964).

²⁷K. Mizuno, A. Matsui, and G. J. Sloan, J. Phys. Soc. Jpn. **53**, 2799 (1984).

²⁸W. Hofberger, Phys. Status Solidi A **34**, K55 (1976).